Physica B 168 (1991) 9–31
North-Holland

The violation of parity and reversality in molecular ensembles

I. Field induced circular and axial birefringence

M.W. Evans[1]

Theory Center, Cornell University, Ithaca, NY 14850, USA

Received 30 January 1990
Revised manuscript received 20 June 1990

The violation of parity and reversality are fundamental phenomena which are investigated using magnetic, electric and electromagnetic field circular and axial birefringence in chiral and achiral molecular ensembles. Symmetry considerations determine whether parity (P) or reversality (T) must be violated in order to observe the circular or axial birefringence spectroscopically. Several types of field induced birefringence are considered, using static and time varying magnetic and electric fields, and intense electromagnetic fields. In each case, the symmetry of the complete experiment is considered, and if P and T are conserved, expressions are derived for the circular and axial refractive and absorption indices in terms of appropriate molecular property tensors. The order of magnitude of each new birefringence effect is estimated, and spectroscopic configurations suggested for their experimental observation.

1. Introduction

One of the most profound realizations of twentieth century physics is that matter is handed at the fundamental level. This means that parity reversal symmetry

$$P(X, Y, Z) = (-X, -Y, -Z) \tag{1}$$

is violated in the universe, and that signs of this should occur in the spectroscopy of molecular ensembles. After the discovery of parity violating optical activity in atomic ensembles [1–3], the search for suitable spectroscopic configurations for the observation of P violation has intensified [4–8] and this paper aims to define P violating spectroscopic configurations in field induced circular and axial birefringence, using chiral and achiral molecular ensembles. One of our aims here is to find a configuration which is particularly sensitive to P violation.

The time reversal operator, T, reverses momenta but leaves positions unchanged [9–13], and is linked to the P operator through the fundamental theorem of Luders et al. [14]:

$$CPT = \text{constant}\,, \tag{2}$$

where C is the charge conjugation operator. Physical laws are invariant to T when reversality is conserved, and this fundamental symmetry principle means that when t is replaced by $-t$ in equations describing these laws, the result should be the same. It also means that when an experimental configuration is established, and the T operator is applied to all the observables and variables, these

[1] Guest of the University of Zurich, Institute of Physical Chemistry, Winterthurerstrasse 190, CH-8067 Zurich, Switzerland (1990/1991).

must bear the same relation to each other in the experiment with all motions reversed. Similarly, the same relative symmetry must be obtained when the P operator is applied. Before the discovery of parity violation in the mid fifties [15] it was taken as axiomatic that all experiments must conserve P and T. It is now known that they need not do so.

The conservation of P and T has been used by Barron [16], for example, to explain why a static electric field cannot induce optical activity in an achiral molecular ensemble, whereas a static magnetic field produces the well-known Faraday effect [16] (rotation of the plane of polarised light). In section 2 of this paper, these "complete experiment" symmetry arguments are applied to field induced circular birefringence, of the Faraday type, and also to new axial birefringence effects, of the type first discovered by Wagnière and Meier [17–19], who found that the refractive and absorption indices of a chiral molecular ensemble are slightly different when observed with unpolarised light parallel and antiparallel to a static magnetic field. This is "axial" birefringence because it occurs in the same (Z) axis as the propagating electromagnetic wave vector ($\boldsymbol{K}$), and was called "magnetochiral" birefringence by Barron and Vrbancich [20]. Section 2 applies the principles of parity and reversality conservation to possible new axial and circular birefringence effects, induced by electric and intense electromagnetic fields.

Section 3 examines new field induced axial and circular birefringence effects which were found from section 2 to conserve P and T. The external fields are assumed to perturb the molecular polarisability and optical activity [21] tensors, and these perturbations are expressed in appropriate Taylor expansions in powers of the field components. In this way the field induced circular and axial birefringence is shown to be mediated by new fundamental molecular property tensors, which provide a great deal of information on the electric and magnetic properties of molecules, and which are in general frequency dependent and complex. The circular and axial absorption and refractive indices induced by the applied field represent, therefore, new types of spectra which conserve P and T. These are of fundamental interest in themselves, but additional fundamental information can be generated in spectroscopic configurations where parity and/or reversality are violated.

Parity violating circular and axial birefringence is treated in section 4 using magnetic, electric, and electromagnetic applied fields which perturb the molecular polarisability and optical activity tensors through P violating molecular property tensors which are also complex and frequency dependent. This introduces the possibility of P violating spectra in appropriate experimental configurations, which are defined by reference to the symmetry arguments of section 2. Similarly, a configuration which violates reversality is considered in terms of the same type of Taylor expansion.

Section 5 develops core equations from which the Taylor expansions of sections 3 and 4 generate expressions for the ensemble-averaged circular and axial birefringence induced by magnetic, electric, and electromagnetic fields. An order of magnitude estimate is made for birefringence effects which conserve P and T, and it is shown that electromagnetic field induced axial birefringence can be orders of magnitude greater than other types. Furthermore, there are several different types of electromagnetic field induced axial and circular birefringence which conserve P and T.

Section 6 defines a class of electromagnetic field induced axial birefringence which violates P, and gives an order of magnitude estimate of the P violating, frequency dependent, birefringence, using the power of a giant ruby laser to maximise the sensitivity of the apparatus to the P violating birefringence and dichroism.

Section 7 similarly isolates a configuration which violates reversality, again using powerful electromagnetic fields to increase experimental sensitivity to the T violating spectrum.

Section 8 is a computer simulation of one of the new electromagnetic field induced axial birefringence effects, providing data on appropriate time correlation functions as the molecular ensemble responds to the applied field.

Finally, section 9 is a discussion of possible experimental configurations and suggestions for further work.

2. Fundamental symmetry: the conservation and violation of parity and reversality

2.1. Magnetic fields

It has been known for nearly 150 years that a static magnetic field rotates the plane of polarised light, producing circular birefringence (the Faraday effect) in both chiral and achiral molecular ensembles. The symmetry of this effect, and that of axial birefringence induced by a static magnetic field, the Wagnière–Meier effect [17–19], is formulated as follows (see appendix A):

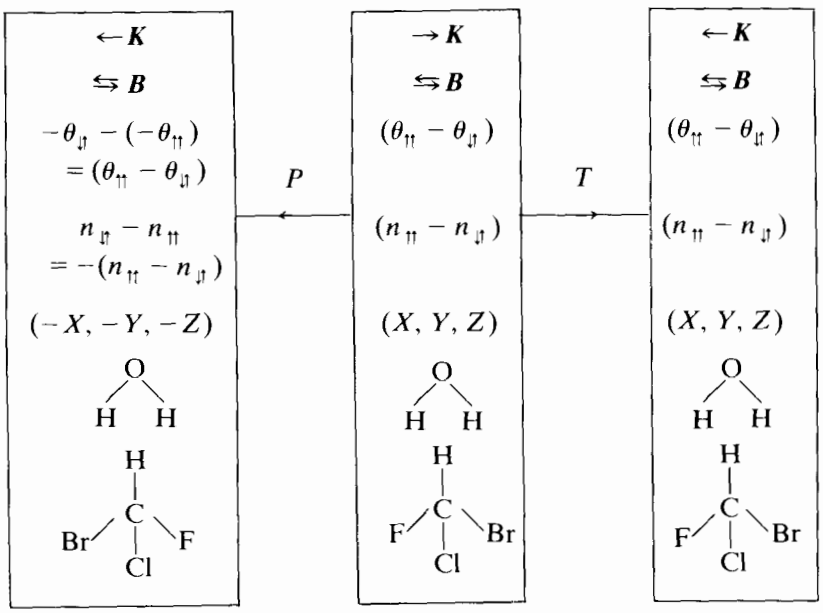

(3)

Here, the effect of T and P is shown on the observables and variables of the Faraday and Wagnière–Meier effects. The observables are defined as follows. $(\theta_{\uparrow\uparrow} - \theta_{\downarrow\uparrow})$ is the difference in the rotation angle of circular birefringence with a static magnetic field, $\boldsymbol{B}$, parallel and antiparallel to the propagation vector, $\boldsymbol{K}$, of the probe electromagnetic radiation. The latter is plane polarised in the Faraday effect and unpolarised in the Wagnière–Meier effect. $(n_{\uparrow\uparrow} - n_{\downarrow\uparrow})$ is the axial refractive (or absorption) index difference of the Wagnière–Meier effect, measured in the same, Z, axis as the unpolarised probe light beam, the latter being parallel or antiparallel to $\boldsymbol{B}$. The final two symbols, representing the water molecule and the simplest chiral molecular framework, represent the effect of T and P on molecular structure. In achiral structures such as water, the T and P operations both conserve the ensemble symmetry; but in chiral ensembles, the P operator takes the ensemble to its enantiomer, thus generating a physically different entity. The operations are carried out in the laboratory frame (X, Y, Z).

The symmetry diagram (3) shows that both the Faraday and the Wagnière–Meier effect conserve T in all ensembles. The observables and variables in the motion-reversed experiment (right-hand panel) bear the same relation to each other. The Faraday effect conserves P in achiral ensembles, but P reverses the sign of $(n_{\uparrow\uparrow} - n_{\downarrow\uparrow})$ because the relative directions of $\boldsymbol{K}$ and $\boldsymbol{B}$ are reversed (left-hand panel of diagram (3)). Thus, the Wagnière–Meier effect violates P in achiral molecular ensembles. However,

it does not do so in chiral ensembles, because the P operation in this case takes the ensemble to a different enantiomer. Chiral molecular ensembles cannot distinguish between odd- and even-parity variables in consequence, and the irreducible representations, $D^{(0)} \cdots D^{(n)}$ of the pure rotation point group $R(3)$ of chiral ensembles [22–26], do not have u (negative parity) or g (positive parity) subscripts. The symmetry panels of diagram (3) show the following:

(1) Circular birefringence produced by a static magnetic field (the Faraday effect) conserves P and T in chiral and achiral ensembles.

(2) Axial birefringence produced by a static magnetic field (the Wagnière–Meier effect) conserves T in all ensembles, but violates P in achiral ensembles.

(3) Circular and axial birefringence produced by a time varying magnetic field violates reversality both in chiral and achiral ensembles, because $\boldsymbol{B}(t)$ is positive to T, which would reverse the signs of both $(\theta_{\uparrow\uparrow} - \theta_{\downarrow\downarrow})$ and $(n_{\uparrow\uparrow} - n_{\downarrow\downarrow})$ while having no effect on the ensemble symmetry. The relation of observables to ensemble is therefore opposite in the motion-reversed experiment when using a time varying magnetic field. We conclude that the observation of an ensemble-averaged circular or axial birefringence with a time varying magnetic field would be an experimental indication of the violation of reversality.

2.2. *Electric fields*

Symmetry diagram (4) summarises the effect of P and t when a static electric field is applied parallel or antiparallel to $\boldsymbol{K}$ of a probe laser:

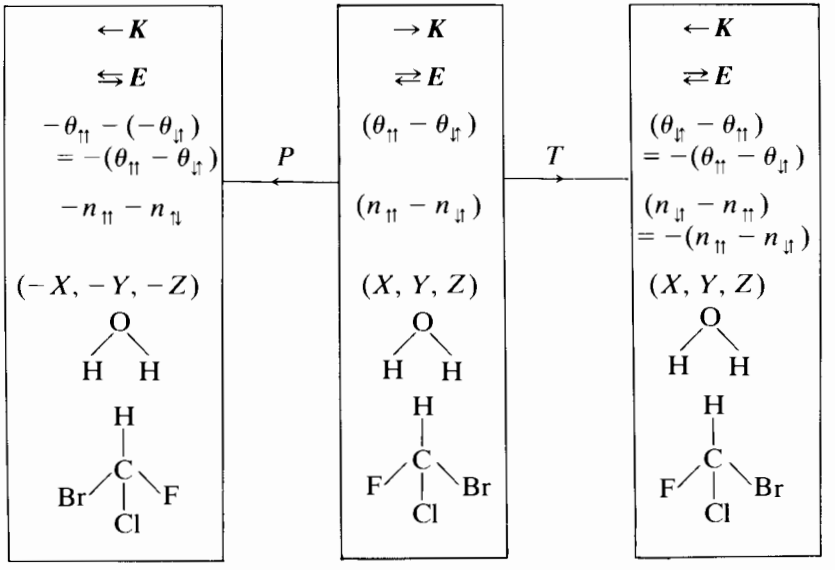

(4)

A static electric field is positive to T, and in consequence the right-hand panel shows that in the motion-reversed experiment the signs of both $(\theta_{\uparrow\uparrow} - \theta_{\downarrow\downarrow})$ and $(n_{\uparrow\uparrow} - n_{\downarrow\downarrow})$ are reversed, while the symmetry of the ensemble (chiral or achiral) is unchanged. In direct analogy with the time varying magnetic field, just discussed, diagram (4) shows the following:

(1) Circular birefringence caused by a static electric field in achiral ensembles violates both T and P.
(2) Axial birefringence caused by a static field violates T in achiral ensembles, but conserves P. This effect isolates, in principle, a spectrum due to reversality violation.
(3) Both axial and circular birefringence caused by a time varying electric field $\dot{E}(t)$ conserve T in both chiral and achiral ensembles. Circular birefringence of this type violates P in achiral ensembles; but the corresponding axial birefringence conserves both P and T in all ensembles.

Both P and T are conserved in consequenced in circular birefringence due to a time varying electric field in chiral ensembles; and in axial birefringence due to a time varying electric field in both achiral and chiral ensembles.

2.3. *Electromagnetic fields*

In this case we consider the symmetry of powerful, circularly polarised, lasers parallel or antiparallel to a weak probe laser. In symmetry diagram (5) the power laser is kept parallel to the probe, and its circular polarisation switched from right to left. In symmetry diagram (6) the polarisation of the power laser is kept the same while its direction is reversed relative to the probe from parallel to antiparallel. Considering diagram (5) firstly:

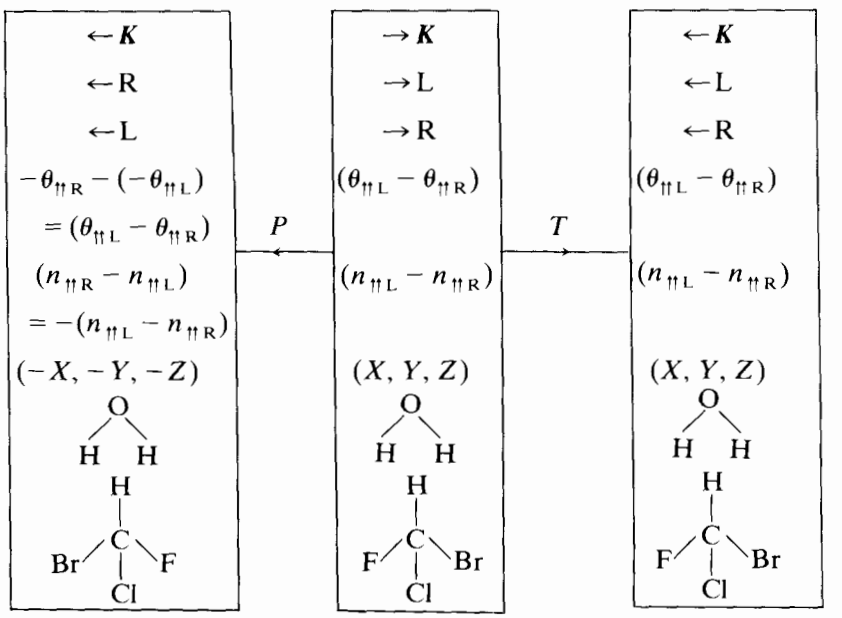

(5)

it is seen that both circular and axial birefringence generated by switching the power laser from right to left, while maintaining its parallel orientation relative to the probe, conserve T in both chiral and achiral ensembles. This is because T reverses the propagation vectors of both lasers (power and probe), while maintaining the handedness of the power laser. The signs of the observables $(\theta_{\uparrow\uparrow L} - \theta_{\uparrow\uparrow R})$ and $(n_{\uparrow\uparrow L} - n_{\uparrow\uparrow R})$ are unchanged in the motion-reversed experiment. The P operation (left-hand panel) leaves $(\theta_{\uparrow\uparrow L} - \theta_{\uparrow\uparrow R})$ unchanged, but reverses the sign of $(n_{\uparrow\uparrow L} - n_{\uparrow\uparrow R})$. We conclude that this type (class one) of "spin chiral" dichroism [27] has the following characteristics (see appendix A).

(1) Class one spin chiral dichroism conserves T in chiral and achiral ensembles, both for circular and for axial birefringence.
(2) It conserves P in all ensembles for circular birefringence, but violates P in achiral ensembles for axial birefringence.

We shall see that this is a potentially sensitive method for the exploration of P violation because of the power levels attainable in a power laser such as the focussed giant ruby laser.

Symmetry diagram (6) demonstrates the P and T symmetries of class two spin chiral dichroism, where the circular polarity of the laser is maintained constant, and where its direction is reversed relative to the probe. This generates both circular and axial birefringence, measured by the probe, as detailed later in this work. Diagram (6) shows the following:

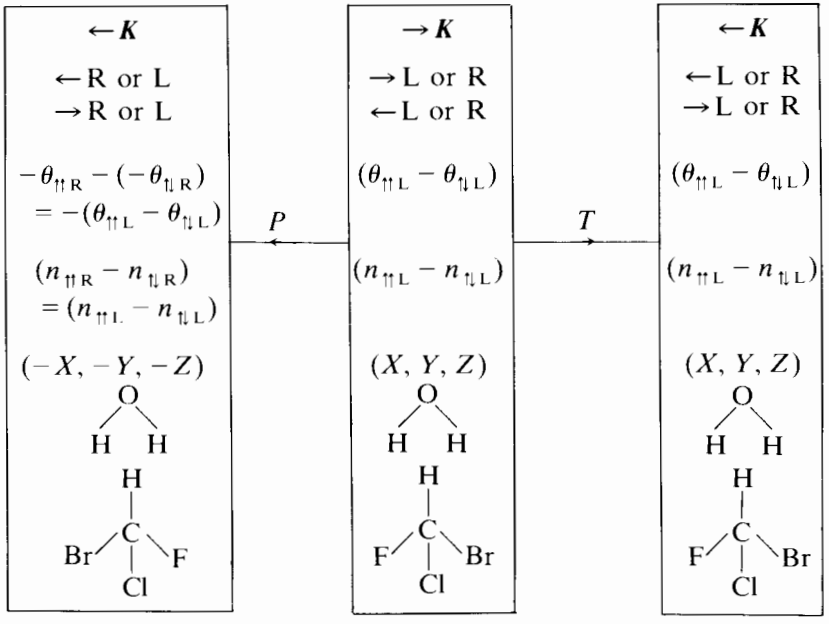

(6)

(1) Both circular and axial birefringence caused by class two spin chiral dichroism conserve T in all ensembles.
(2) Circular birefringence in class two violates P in achiral ensembles, but axial birefringence of the same class conserves P in all ensembles. This is an opposite parity symmetry to class one. Thus, the observation of circular birefringence in class two configuration would be a P violating spectrum. Again, the power of a focussed giant ruby laser pulse train makes this a particularly sensitive method for the detection of P violation in achiral molecular ensembles.

3. *P* and *T* conserving phenomena, Taylor expansions of the polarisability and optical activity tensors

3.1. Magnetic fields

It is assumed, following Barron and Vrbancich [20], that the rank two molecular polarisability and optical activity tensors can be expanded in Taylor series in powers of the static magnetic flux density $\boldsymbol{B}$:

$$\alpha_{1ij}(\boldsymbol{B}) = \alpha_{1ij} + \left(\frac{\partial \alpha_{1ij}}{\partial B_k}\right)_0 B_k + \frac{1}{2!}\left(\frac{\partial^2 \alpha_{1ij}}{\partial B_k\, \partial B_l}\right)_0 B_k B_l + \cdots , \tag{7}$$

$$\alpha_{2ij}(\boldsymbol{B}) = \alpha_{2ij} + \left(\frac{\partial \alpha_{2ij}}{\partial B_k}\right)_0 B_k + \frac{1}{2!}\left(\frac{\partial^2 \alpha_{2ij}}{\partial B_k\, \partial B_l}\right)_0 B_k B_l + \cdots . \tag{8}$$

Here $\alpha_{1ij}(\boldsymbol{B})$ is the magnetic field dependent molecular polarisability tensor; $\alpha_{2ij}(\boldsymbol{B})$ the $\boldsymbol{B}$ dependent optical activity tensor, and the Taylor expansions define higher rank perturbing tensors such as

$$\alpha^{(B)}_{1ijk} \equiv \left(\frac{\partial \alpha_{1ij}}{\partial B_k}\right)_0 , \qquad \alpha^{(B)}_{2ijk} \equiv \left(\frac{\partial \alpha_{2ij}}{\partial B_k}\right)_0 . \tag{9}$$

All tensors conserve P and T, meaning that they contain no intrinsic P or T violating components. In general, all are frequency dependent and complex, for example,

$$\alpha^{(B)}_{1ijk} \equiv \alpha^{(B)\prime}_{1ijk} + \mathrm{i}\alpha^{(B)\prime\prime}_{1ijk} , \tag{10}$$

where single primes denote real parts and double primes denote imaginary parts. Confining the Taylor expansion to first order in B gives the perturbation expressions used by Barron and Vrbancich [20]:

$$\alpha_{1ij}(\boldsymbol{B}) = \alpha_{1ij} \pm \alpha^{(B)}_{1ijZ} B_Z , \tag{11}$$

$$\alpha_{2ij}(\boldsymbol{B}) = \alpha_{2ij} \pm \alpha^{(B)}_{2ijZ} B_Z , \tag{12}$$

where the plus sign denotes $\boldsymbol{B}$ in the $+Z$ direction and the minus sign denotes $\boldsymbol{B}$ in the $-Z$ direction. Note that the third rank tensor $\alpha^{(B)}_{1ijk}$ mediating the effect of $\boldsymbol{B}$ on molecular polarisability is positive to P, and is suported by achiral ensembles. The tensor $\alpha^{(B)}_{2ijk}$ mediating the effect of $\boldsymbol{B}$ on the negative-parity optical activity tensor α_{2ij} is also negative to P, and is supported only in chiral ensembles. The core equations of section 5 show that the Faraday effect depends on $\alpha^{(B)}_{1ijk}$ and the Wagnière–Meier effect depends on $\alpha^{(B)}_{2ijk}$. This is consistent with the symmetry analysis of section 2.

3.2. *Sinusoidal time varying electric field, $\dot{\boldsymbol{E}}(t)$*

Section 2 has shown that P and T conserving circular and axial birefringence is supported only by a time varying electric field. This is assumed to make the polarisability and optical activity tensors functions of $\dot{\boldsymbol{E}}(t)$, functions which are expanded in the following Taylor series:

$$\alpha_{1ij}(\dot{\boldsymbol{E}}(t)) = \alpha_{1ij} \pm \alpha^{(E)}_{1ijZ} \dot{E}_Z(t) , \tag{13}$$

$$\alpha_{2ij}(\dot{\boldsymbol{E}}(t)) = \alpha_{2ij} \pm \alpha^{(E)}_{2ijZ} \dot{E}_Z(t) , \tag{14}$$

with higher rank molecular property tensors mediating the effect of each power of $\dot{\boldsymbol{E}}(t)$. These are defined similarly to their magnetic field counter parts and are also complex and frequency dependent quantities in general. This time the rank three tensor mediating the effect of a sinusoidal $\dot{\boldsymbol{E}}(t)$ on α_{1ij} is an odd-parity tensor, supported only in chiral ensembles, and its counterpart $\alpha^{(E)}_{2ijk}$, mediating the effect of $\dot{\boldsymbol{E}}(t)$ on α_{2ij}, is even parity, supported in achiral ensembles. To first order in $\dot{\boldsymbol{E}}(t)$, the core equations of section 5 show that these third rank tensors are the ones responsible respectively for circular and axial birefringence due to a time varying electric field.

3.3. Electromagnetic field

In this case the tensors α_{1ij} and α_{2ij} become functions of both electric and magnetic components, $\boldsymbol{E}^{(\mathrm{p})}$ and $\boldsymbol{B}^{(\mathrm{p})}$, respectively, of the electromagnetic field of the power laser, denoted by superscript (p) to distinguish it from the probe light beam. With a similar expression for $\alpha_{2ij}(\boldsymbol{E}^{(\mathrm{p})}, \boldsymbol{B}^{(\mathrm{p})})$, the polarisability tensor $\alpha_{1ij}(\boldsymbol{E}^{(\mathrm{p})}, \boldsymbol{B}^{(\mathrm{p})})$ is expanded in the following two variable Taylor series to second order:

$$\alpha_{1ij}(\boldsymbol{E}^{(\mathrm{p})}, \boldsymbol{B}^{(\mathrm{p})}) = \alpha_{1ij} + \alpha^{(1)}_{1ijk} E^{(\mathrm{p})}_k + \alpha^{(2)}_{1ijk} B^{(\mathrm{p})}_k + \frac{1}{2!}\left[\alpha^{(3)}_{1ijkl} E^{(\mathrm{p})}_k E^{(\mathrm{p})}_l + \alpha^{(4)}_{1ijkl} B^{(\mathrm{p})}_k E^{(\mathrm{p})}_l + \alpha^{(5)}_{1ijkl} E_k B_l + \alpha^{(6)}_{1ijkl} B_k B_l\right] + \cdots, \tag{15}$$

where the third and fourth rank mediating tensors are defined as follows:

$$\alpha^{(1)}_{1ijk} \equiv \frac{\partial \alpha_{1ij}}{\partial E^{(\mathrm{p})}_k}, \qquad \alpha^{(2)}_{1ijk} = \frac{\partial \alpha_{1ij}}{\partial B^{(\mathrm{p})}_k},$$

$$\alpha^{(3)}_{1ijkl} \equiv \frac{\partial}{\partial E^{(\mathrm{p})}_k}\left(\frac{\partial \alpha_{1ij}}{\partial E^{(\mathrm{p})}_l}\right), \qquad \alpha^{(4)}_{1ijkl} \equiv \frac{\partial}{\partial E^{(\mathrm{p})}_k}\left(\frac{\partial \alpha_{1ij}}{\partial B^{(\mathrm{p})}_l}\right),$$

and so on. All tensors intrinsically conserve P and T, i.e. they do not contain P or T violating components, because we are looking at phenomena which conserve P and T overall, as defined in section 2. In general, these are all complex and frequency dependent molecular properties. Equation (15) shows that there are a variety of possible new circular and axial birefringence effects due to a power laser. Section 5 considers two of these in detail, second order effects responsible for the class one and class two spin chiral symmetries considered in section 2.

4. Parity violating field induced birefringence

This section considers P violating birefringence defined by configurations taken from section 2. In particular, P violating birefringence due to class one and class two spin chiral effects are considered, because the power levels and field intensities of a focussed giant ruby laser maximise the sensitivity of the apparatus to the intrinsically P violating tensors considered in this section. It is assumed that there exist intrinsically P violating molecular property tensors akin to those in section 3. These conserve reversality. They are distinguished from their P conserving counterparts by the subscript PV. The P violating counterpart of eq. (15) becomes

$$[\alpha_{1ij}(\boldsymbol{E}^{(\mathrm{p})}, \boldsymbol{B}^{(\mathrm{p})})]_{\mathrm{PV}} = [\alpha_{1ij}]_{\mathrm{pv}} + [\alpha^{(1)}_{1ijk}]_{\mathrm{PV}} E^{(\mathrm{p})}_k + [\alpha^{(2)}_{1ijk}]_{\mathrm{PV}} B^{(\mathrm{p})}_k + \frac{1}{2!}\left[[\alpha^{(3)}_{1ijkl}]_{\mathrm{PV}} E^{(\mathrm{p})}_k E^{(\mathrm{p})}_l + \cdots\right] + \cdots, \tag{16}$$

and for the parity violating counterpart of the optical activity tensor,

$$[\alpha_{2ij}(\boldsymbol{E}^{(\mathrm{p})}, \boldsymbol{B}^{(\mathrm{p})})]_{\mathrm{PV}} = [\alpha_{2ij}]_{\mathrm{PV}} + [\alpha^{(1)}_{2ijk}]_{\mathrm{PV}} E^{(\mathrm{p})}_k + [\alpha^{(2)}_{2ijk}]_{\mathrm{PV}} B^{(\mathrm{p})}_k + \frac{1}{2!}\left[[\alpha^{(3)}_{2ijkl}]_{\mathrm{PV}} E^{(\mathrm{p})}_k E^{(\mathrm{p})}_l + \cdots\right] + \cdots, \tag{17}$$

$$\alpha_{1ij}(\boldsymbol{B}) = \alpha_{1ij} + \left(\frac{\partial \alpha_{1ij}}{\partial B_k}\right)_0 B_k + \frac{1}{2!}\left(\frac{\partial^2 \alpha_{1ij}}{\partial B_k \, \partial B_l}\right)_0 B_k B_l + \cdots , \tag{7}$$

$$\alpha_{2ij}(\boldsymbol{B}) = \alpha_{2ij} + \left(\frac{\partial \alpha_{2ij}}{\partial B_k}\right)_0 B_k + \frac{1}{2!}\left(\frac{\partial^2 \alpha_{2ij}}{\partial B_k \, \partial B_l}\right)_0 B_k B_l + \cdots . \tag{8}$$

Here $\alpha_{1ij}(\boldsymbol{B})$ is the magnetic field dependent molecular polarisability tensor; $\alpha_{2ij}(\boldsymbol{B})$ the $\boldsymbol{B}$ dependent optical activity tensor, and the Taylor expansions define higher rank perturbing tensors such as

$$\alpha^{(B)}_{1ijk} \equiv \left(\frac{\partial \alpha_{1ij}}{\partial B_k}\right)_0 , \qquad \alpha^{(B)}_{2ijk} \equiv \left(\frac{\partial \alpha_{2ij}}{\partial B_k}\right)_0 . \tag{9}$$

All tensors conserve P and T, meaning that they contain no intrinsic P or T violating components. In general, all are frequency dependent and complex, for example,

$$\alpha^{(B)}_{1ijk} \equiv \alpha^{(B)\prime}_{1ijk} + \mathrm{i}\alpha^{(B)\prime\prime}_{1ijk} , \tag{10}$$

where single primes denote real parts and double primes denote imaginary parts. Confining the Taylor expansion to first order in B gives the perturbation expressions used by Barron and Vrbancich [20]:

$$\alpha_{1ij}(\boldsymbol{B}) = \alpha_{1ij} \pm \alpha^{(B)}_{1ijZ} B_Z , \tag{11}$$

$$\alpha_{2ij}(\boldsymbol{B}) = \alpha_{2ij} \pm \alpha^{(B)}_{2ijZ} B_Z , \tag{12}$$

where the plus sign denotes $\boldsymbol{B}$ in the $+Z$ direction and the minus sign denotes $\boldsymbol{B}$ in the $-Z$ direction. Note that the third rank tensor $\alpha^{(B)}_{1ijk}$ mediating the effect of $\boldsymbol{B}$ on molecular polarisability is positive to P, and is suported by achiral ensembles. The tensor $\alpha^{(B)}_{2ijk}$ mediating the effect of $\boldsymbol{B}$ on the negative-parity optical activity tensor α_{2ij} is also negative to P, and is supported only in chiral ensembles. The core equations of section 5 show that the Faraday effect depends on $\alpha^{(B)}_{1ijk}$ and the Wagnière–Meier effect depends on $\alpha^{(B)}_{2ijk}$. This is consistent with the symmetry analysis of section 2.

3.2. *Sinusoidal time varying electric field, $\dot{\boldsymbol{E}}(t)$*

Section 2 has shown that P and T conserving circular and axial birefringence is supported only by a time varying electric field. This is assumed to make the polarisability and optical activity tensors functions of $\dot{\boldsymbol{E}}(t)$, functions which are expanded in the following Taylor series:

$$\alpha_{1ij}(\dot{\boldsymbol{E}}(t)) = \alpha_{1ij} \pm \alpha^{(E)}_{1ijZ} \dot{E}_Z(t) , \tag{13}$$

$$\alpha_{2ij}(\dot{\boldsymbol{E}}(t)) = \alpha_{2ij} \pm \alpha^{(E)}_{2ijZ} \dot{E}_Z(t) , \tag{14}$$

with higher rank molecular property tensors mediating the effect of each power of $\dot{\boldsymbol{E}}(t)$. These are defined similarly to their magnetic field counter parts and are also complex and frequency dependent quantities in general. This time the rank three tensor mediating the effect of a sinusoidal $\dot{\boldsymbol{E}}(t)$ on α_{1ij} is an odd-parity tensor, supported only in chiral ensembles, and its counterpart $\alpha^{(E)}_{2ijk}$, mediating the effect of $\dot{\boldsymbol{E}}(t)$ on α_{2ij}, is even parity, supported in achiral ensembles. To first order in $\dot{\boldsymbol{E}}(t)$, the core equations of section 5 show that these third rank tensors are the ones responsible respectively for circular and axial birefringence due to a time varying electric field.

in which each term violates P intrinsically. It was shown in section 2 that class one spin chiral dichroism violates P in achiral ensembles for axial birefringence, which can exist in achiral ensembles, accordingly, only if mediated by the $[\alpha^{(3)}_{2ijkl}]_{PV}$ tensor of eq. (17). Similarly, class two spin chiral dichroism violates P in achiral ensembles for circular dichroism, which can exist in these ensembles only if mediated by the parity violating tensor $[\alpha^{(4)}_{2ijkl}]_{PV}$. The mechanisms for these effects are deduced from the core equations of section 5 in section 6.

5. The core equations

In this section, core equations are derived which allow the calculation of axial and circular refractive and absorption indices induced by external fields. These indices give the complex permittivity and power absorption coefficients directly. They are derived from Maxwell's equation (see appendix B).

$$\frac{1}{\mu_0}\nabla\times\boldsymbol{B}^{(1)}=\epsilon_0\frac{\partial\boldsymbol{E}^{(1)}}{\partial t}+\frac{\partial N}{\partial t}(\alpha_{1ij}E_j^{(1)}+\alpha_{2ij}B_j^{(1)}), \tag{18}$$

where μ_0 denotes the permeability and ϵ_0 the permittivity of free space, $\boldsymbol{B}^{(1)}$ is the magnetic field and $\boldsymbol{E}^{(1)}$ the electric field component of the probe light beam:

$$\begin{aligned}\boldsymbol{E}_L^{(1)}&=E_0^{(1)}(\boldsymbol{i}-\mathrm{i}\boldsymbol{j})\,\mathrm{e}^{\mathrm{i}\phi_L}, \qquad \boldsymbol{B}_L^{(1)}=B_0^{(1)}(\boldsymbol{j}+\mathrm{i}\boldsymbol{i})\,\mathrm{e}^{\mathrm{i}\phi_L},\\ \boldsymbol{E}_R^{(1)}&=E_0^{(1)}(\boldsymbol{i}+\mathrm{i}\boldsymbol{j})\,\mathrm{e}^{\mathrm{i}\phi_R}, \qquad \boldsymbol{B}_R^{(1)}=B_0^{(1)}(\boldsymbol{j}-\mathrm{i}\boldsymbol{i})\,\mathrm{e}^{\mathrm{i}\phi_R},\end{aligned} \tag{19}$$

where the subscripts L and R denote left and right circularly polarised, respectively, and the phases are defined as usual in IUPAC convention as

$$\phi_R=\omega t-\boldsymbol{K}_R\cdot\boldsymbol{r}, \qquad \phi_L=\omega t-\boldsymbol{K}_L\cdot\mathbf{r}. \tag{20}$$

It is assumed that the wave vector is in general a complex quantity, related to the complex refractive index by

$$(\boldsymbol{K}_L'+\mathrm{i}\boldsymbol{K}_L'')=\frac{\omega}{c}(\boldsymbol{n}_L'+\mathrm{i}\boldsymbol{n}_L''),(\boldsymbol{K}_R'+\mathrm{i}\boldsymbol{K}_R'')=\frac{\omega}{c}(\boldsymbol{n}_R'+\mathrm{i}\boldsymbol{n}_R''). \tag{21}$$

With these definitions, eq. (18) can be rewritten as

$$(n_L'+\mathrm{i}n_L'')_Z(\boldsymbol{i}-\mathrm{i}\boldsymbol{j})\frac{B_0^{(1)}}{\mu_0 c}=\epsilon_0E_0^{(1)}(\boldsymbol{i}-\mathrm{i}\boldsymbol{j})+(\alpha_{1ij}E_j^{(1)}+\alpha_{2ij}B_j^{(1)})N \tag{22}$$

and

$$(n_R'+\mathrm{i}n_R'')Z(\boldsymbol{i}+\mathrm{i}\boldsymbol{j})\frac{B_0^{(1)}}{\mu_0 c}=\epsilon_0E_0^{(1)}(\boldsymbol{i}+\mathrm{i}\boldsymbol{j})+(\alpha_{1ij}E_j^{(1)}+\alpha_{2ij}B_j^{(1)})N \tag{23}$$

for the complex refractive index in left and right circularly polarised probe radiation, respectively. In both these equations, the polarisability and optical activity tensors are also complex quantities in general,

$$\alpha_{1ij}\equiv\alpha'_{1ij}+\mathrm{i}\alpha''_{1ij}, \tag{24}$$

$$\alpha_{2ij}\equiv\alpha'_{2ij}+\mathrm{i}\alpha''_{2ij}. \tag{25}$$

Comparing the coefficients of the unit vector $\boldsymbol{i}$ (in the X axis) of eqs. (22) and (23) gives

$$\frac{B_0^{(1)}}{\mu_0 c}(n'_{\mathrm{L}} + \mathrm{i}n''_{\mathrm{L}})_Z = \epsilon_0 E_0^{(1)} + E_0^{(1)}(\alpha_{1XX} - \mathrm{i}\alpha_{1XY})N + B_0^{(1)}(\mathrm{i}\alpha_{2XX} + \alpha_{2XY})N\,, \tag{26}$$

$$\frac{B_0^{(1)}}{\mu_0 c}(n'_{\mathrm{R}} + \mathrm{i}n''_{\mathrm{R}})_Z = \epsilon_0 E_0^{(1)} + E_0^{(1)}(\alpha_{1XX} + \mathrm{i}\alpha_{1XY})N - \beta_0^{(1)}(\mathrm{i}\alpha_{2XX} - \alpha_{2XY})N\,. \tag{27}$$

Comparing the real coefficients in this equation gives

$$n'_{\mathrm{L}Z}\frac{B_0^{(1)}}{\mu_0 c} = \epsilon_0 E_0^{(1)} + [E_0^{(1)}(\alpha'_{1XX} + \alpha''_{1XY}) + B_0^{(1)}(\alpha'_{2XY} - \alpha''_{2XX})]N\,, \tag{28}$$

$$n'_{\mathrm{R}Z}\frac{B_0^{(1)}}{\mu_0 c} = \epsilon_0 E_0^{(1)} + [E_0^{(1)}(\alpha'_{1XX} - \alpha''_{1XY}) + B_0^{(1)}(\alpha'_{2XY} + \alpha''_{2XX})]N\,, \tag{29}$$

for the refractive index in left and right circularly polarised probe radiation, respectively; and comparing the imaginary coefficients gives the absorption indices:

$$n''_{\mathrm{L}Z}\frac{B_0^{(1)}}{\mu_0 c} = [E_0^{(1)}(\alpha''_{1XX} - \alpha'_{1XY}) + B_0^{(1)}(\alpha''_{2XY} + \alpha'_{2XX})]N\,, \tag{30}$$

$$n''_{\mathrm{R}Z}\frac{B_0^{(1)}}{\mu_0 c} = [E_0^{(1)}(\alpha''_{1XX} + \alpha'_{1XY}) + B_0^{(1)}(\alpha''_{2XY} - \alpha'_{2XX})]N\,. \tag{31}$$

5.1. *Axial birefringence*

In this case the probe is unpolarised, and measures the average of the L and R refractive and absorption indices, given by the core equations for axial birefringence:

$$n'_{\mathrm{av}Z} = \frac{\mu_0 c}{B_0^{(1)}}(\epsilon_0 E_0^{(1)} + NE_0^{(1)}\alpha'_{1XX} + NB_0^{(1)}\alpha'_{2XY})\,, \tag{32}$$

$$n''_{\mathrm{av}Z} = \frac{\mu_0 cN}{B_0^{(1)}}(E_0^{(1)}\alpha''_{1XX} + B_0^{(1)}\alpha''_{2XY})\,. \tag{33}$$

The power absorption coefficient in neper cm^{-1}, the ordinate of axial dichroism, is obtained directly from eq. (33) as

$$A_{\mathrm{av}Z}^{\mathrm{axial}}(\mathrm{neper\ cm^{-1}}) = \frac{2\omega\mu_0 N}{B_0^{(1)}}(E_0^{(1)}\alpha''_{1XX} + B_0^{(1)}\alpha''_{2XY}) \tag{34}$$

and the real and imaginary parts of the complex permittivity are obtained from

$$\epsilon' = n'^2 - n''^2\,, \qquad \epsilon'' = 2n''n'\,. \tag{35}$$

5.2. *Circular birefringence*

These are obtained similarly as

$$(n'_{LZ} - n'_{RZ} = 2\mu_0 cN\left[\frac{E_0^{(1)}}{B_0^{(1)}}\,\alpha''_{1XY} - \alpha''_{2XX}\right] \tag{36}$$

and

$$(n''_{LZ} - n''_{RZ}) = 2\mu_0 cN\left[\alpha'_{2XX} - \frac{E_0^{(1)}}{B_0^{(1)}}\,\alpha'_{1XY}\right], \tag{37}$$

i.e. these are expressions for the difference in refractive index in left and right circularly polarised probe radiation. The corresponding power absorption coefficient of circular dichroism is

$$A_Z^{\text{circ}} = 4\omega\mu_0 N\left[\alpha'_{2XX} - \frac{E_0^{(1)}}{B_0^{(1)}}\,\alpha'_{1XY}\right] \tag{38}$$

and the angle of rotation of a plane polarised probe is

$$\Theta = l\mu_0 N\omega\left[\frac{E_0^{(1)}}{B_0^{(1)}}\,\alpha''_{1XY} - \alpha_{2XX}\right], \tag{39}$$

where l is the sample length in meters. The dependence of the angle on the angular frequency ω is the optical rotatory dispersion.

5.3. *Field induced axial and circular birefringence*

These core equations are used in this subsection to relate field induced birefringence effects directly to ensemble-averaged molecular property tensors of the type described in section 3. This is carried out for an external static magnetic field; an external time varying electric field, and for class one and class two spin chiral axial and circular dichroism.

5.3.1. *Static magnetic field* B_Z

Using eqs. (11) and (12) with the core equations for axial and circular birefringence/dichroism, eqs. (32) to (39), gives the following expressions for ensemble-averaged [16] measurables as a function of the mediating tensor elements which survive isotropic averaging [16–19], the totally antisymmetric elements of the third rank tensors $\alpha^{(B)}_{1ijk}$ and $\alpha^{(B)}_{2ijk}$.

The difference between ensemble-averaged refractive indices parallel and antiparallel to the externally applied static magnetic field B_Z is the Wagnière–Meier effect [17–19]:

$$\langle (n_{\uparrow\uparrow} - n_{\uparrow\downarrow})_{B_Z}\rangle = 2\mu_0 cNB_Z\langle \alpha^{(B)\prime}_{2XYZ}\rangle\,. \tag{40}$$

In accordance with the basic symmetry arguments of section 2, this depends on an odd-parity totally antisymmetric tensor element $\langle \alpha^{(B)\prime}_{2XYZ}\rangle$ and conserves parity only in chiral ensembles. It is proportional to B_Z to first order in eq. (8).

The corresponding difference in the power absorption coefficient is

$$\langle A^{\text{axial}}_{\uparrow\uparrow} - A^{\text{axial}}_{\uparrow\downarrow}\rangle = 4\mu_0 N\omega B_Z\langle \alpha^{(B)\prime\prime}_{2XYZ}\rangle \tag{41}$$

and depends on the imaginary component of the odd parity tensor, $\langle \alpha^{(B)\prime\prime}_{2XYZ}\rangle$. This is the axial dichroism of the Wagnière–Meier effect, and is proportional to the angular frequency, ω, of the probe radiation. Axial dichroism of this nature conserves parity in chiral ensembles only.

The corresponding circular birefringence induced by B_Z, the Faraday effect, is given in this treatment by

$$\langle(\theta_{\uparrow\uparrow} - \theta_{\uparrow\downarrow})_{B_Z}\rangle = 4\mu_0 cN \frac{E_0^{(1)}}{B_0^{(1)}} B_Z \langle \alpha_{1XYZ}^{(B)\prime\prime}\rangle , \tag{42}$$

where

$$E_0^{(1)} = \epsilon_0'^{1/2} c B_0^{(1)} , \tag{43}$$

with ϵ_0' as the static permittivity of free space, and where

$$V = l\mu_0 N\omega\epsilon_0'^{1/2} c \langle \alpha_{1XYZ}^{(B)\prime\prime}\rangle \tag{44}$$

is the Verdet constant. It is seen that the Faraday effect depends on the even-parity, totally antisymmetric, tensor component $\langle \alpha_{1XYZ}^{(B)\prime\prime}\rangle$ and therefore conserves parity in both achiral and chiral ensembles in accordance with section 2. The corresponding circular dichroism in the power absorption coefficient is

$$\langle(A_{\uparrow\uparrow}^{\text{circ}} - A_{\uparrow\downarrow}^{\text{circ}})\rangle = -8\omega\mu_0 N\epsilon_0'^{1/2} c B_Z \langle \alpha_{1XYZ}^{(B)\prime}\rangle \tag{45}$$

and the rotation of the plane of polarised radiation is

$$\langle(\Theta_{\uparrow\uparrow} - \Theta_{\uparrow\downarrow})_{B_Z}\rangle = 2l\mu_0 N\omega\epsilon_0'^{1/2} c B_Z \langle \alpha_{1XYZ}^{(B)\prime\prime}\rangle . \tag{46}$$

5.3.2. Time varying electric field, $\dot{E}_Z(t)$

Using eqs. (13) and (14) in the core equations provides the following measurables in terms of nonvanishing, totally antisymmetric, elements of the ensemble-averaged mediating tensors $\alpha_{1ijk}^{(E)}$ and $\alpha_{2ijk}^{(E)}$.

The axial birefringence due to the time varying electric field is

$$\langle(n_{\uparrow\uparrow} - n_{\uparrow\downarrow})_{E_Z(t)}\rangle = 2\mu_0 cN\dot{E}_Z(t)\langle \alpha_{2XYZ}^{(E)\prime}\rangle , \tag{47}$$

which is proportional to the even-parity ensemble average and which therefore conserves parity and reversality in achiral and chiral ensembles. This measurable is generated by switching the direction of $\dot{E}_Z(t)$ from $+Z$ to $-Z$.

The corresponding axial dichroism in the power absorption coefficient is

$$\langle(A_{\uparrow\uparrow}^{\text{axial}} - A_{\uparrow\downarrow}^{\text{axial}})_{E_Z(t)}\rangle = 4\mu_0 N\omega\dot{E}_Z(t)\langle \alpha_{2XYZ}^{(E)\prime\prime}\rangle , \tag{48}$$

which again conserves parity and reversality in achiral and chiral ensembles. These results are again in accordance with the fundamental symmetry arguments of section 2.

The circular birefringence due to $\dot{E}_Z(t)$ is

$$\langle(\theta_{\uparrow\uparrow} - \theta_{\uparrow\downarrow})_{E_Z(t)}\rangle = 4\mu_0 Nc^2\epsilon_0'^{1/2}\dot{E}_Z(t)\langle \alpha_{1XYZ}^{(E)\prime\prime}\rangle , \tag{49}$$

which depends on the odd-parity tensor element $\langle \alpha_{1XYZ}^{(E)\prime\prime}\rangle$, and therefore conserves parity and reversality only in chiral ensembles.

The corresponding circular dichroism is

$$\langle (A^{\text{circ}}_{\Uparrow\Uparrow} - A^{\text{circ}}_{\Uparrow\Downarrow})_{E_Z(t)} \rangle = -8\omega\mu_0 N\epsilon_0'^{1/2} c\dot{E}_Z(t) \langle \alpha^{(E)\prime}_{1XYZ} \rangle \,, \tag{50}$$

and the difference in the rotation angle on switching $E_Z(t)$ from $+Z$ to $-Z$ is

$$\langle (\Theta_{\Uparrow\Uparrow} - \Theta_{\Uparrow\Downarrow})_{E_Z(t)} \rangle = 2l\mu_0 N\omega\epsilon_0'^{1/2} c\dot{E}_Z(t) \langle \alpha^{(E)\prime\prime}_{1XYZ} \rangle \,. \tag{51}$$

Both of these variables conserve parity only in chiral ensembles.

5.3.3. Class one spin chiral effects

Class one spin chiral effects conserve reversality as discussed in section 2. They are exemplified here by the

$$\alpha_{1ij}(\boldsymbol{E}^{(\mathrm{p})}) = \alpha_{1ij} + \frac{1}{2!}\, \alpha^{(3)}_{1ijkl} E^{(\mathrm{p})}_k E^{(\mathrm{p})}_l \tag{52}$$

term of the two-variable Taylor expansion of the polarisability, eq. (15), and by its counterpart

$$\alpha_{2ij}(\boldsymbol{E}^{(\mathrm{p})}) = \alpha_{2ij} + \frac{1}{2!}\, \alpha^{(3)}_{2ijkl} E^{(\mathrm{p})}_k E^{(\mathrm{p})}_l \tag{53}$$

for the optical rotation tensor α_{2ij}.

The symmetry of the tensor product $E^{(\mathrm{p})}_k E^{(\mathrm{p})}_l$ of power laser electric field components can be represented as follows in terms of the irreducible D representations [28] of the point groups $R_{\mathrm{h}}(3)$ of achiral ensembles and $R(3)$ of chiral ensembles:

$$R_{\mathrm{h}}(3)\colon \Gamma(E^{(\mathrm{p})}_k E^{(\mathrm{p})}_l) = D^{(0)}_{\mathrm{g}} + D^{(1)}_{\mathrm{g}} + D^{(2)}_{\mathrm{g}} \,, \tag{54}$$

$$R(3)\colon \Gamma(E^{(\mathrm{p})}_k E^{(\mathrm{p})}_l) = D^{(0)} + D^{(1)} + D^{(2)} \,. \tag{55}$$

The $D^{(1)}_{\mathrm{g}}$ or $D^{(1)}$ part of these symmetry representations symbolises the rank one tensor (i.e. vector) generated by the vector (cross) product $E^{(\mathrm{p})}_k \times E^{(\mathrm{p})}_l$. Writing out the two complex conjugates, respectively, of the right and left circularly polarised electric field components of the power laser,

$$\left.\begin{aligned} \boldsymbol{E}^{+(\mathrm{p})}_{\mathrm{R}} &= E^{(\mathrm{p})}_0 (\boldsymbol{i} - \mathrm{i}\boldsymbol{j})\, \mathrm{e}^{\mathrm{i}\phi_{\mathrm{R}}}, \qquad \boldsymbol{E}^{-(\mathrm{p})}_{\mathrm{R}} = E^{(\mathrm{p})}_0 (\boldsymbol{i} + \mathrm{i}\boldsymbol{j})\, \mathrm{e}^{-\mathrm{i}\phi_{\mathrm{R}}} \,; \\ \boldsymbol{E}^{+(\mathrm{p})}_{\mathrm{L}} &= E^{(\mathrm{p})}_0 (\boldsymbol{i} + \mathrm{i}\boldsymbol{j})\, \mathrm{e}^{\mathrm{i}\phi_{\mathrm{L}}}, \qquad \boldsymbol{E}^{-(\mathrm{p})}_{\mathrm{L}} = E^{(\mathrm{p})}_0 (\boldsymbol{i} - \mathrm{i}\boldsymbol{j})\, \mathrm{e}^{-\mathrm{i}\phi_{\mathrm{L}}} \,, \end{aligned}\right\} \tag{56}$$

it is possible to form the conjugate products

$$\boldsymbol{\Pi}_1 = \boldsymbol{E}^{+(\mathrm{p})}_{\mathrm{L}} \times \boldsymbol{E}^{-(\mathrm{p})}_{\mathrm{L}} = -\boldsymbol{E}^{+(\mathrm{p})}_{\mathrm{R}} \times \boldsymbol{E}^{-(\mathrm{p})}_{\mathrm{R}} = 2E^{(\mathrm{p})2}_0 \mathrm{i}\boldsymbol{k} \tag{57}$$

responsible for the electric rectification phenomenon [29] of nonlinear optics. The conjugate product (57) reverses sign from $+Z$ to $-Z$ as the circular polarity of the power laser is switched from left to right. The effect of this is picked up as axial and circular birefringence by the probe laser, directed along the same Z axis as the power laser. Writing the product (57) in the tensor notation,

$$2E^{(\mathrm{p})2}_0 \mathrm{i}\boldsymbol{k} \equiv (2E^{(\mathrm{p})2}_0)_Z \mathrm{i} \,, \tag{58}$$

eqs. (52) and (53) become

$$\left.\begin{aligned}\alpha'_{1ij}(\boldsymbol{E}_{\mathrm{p}}) &= \alpha'_{1ij} \mp \alpha^{(3)\prime\prime}_{1ijZ}(E_0^{(\mathrm{p})2})_Z \,, \\ \alpha''_{1ij}(\boldsymbol{E}_{\mathrm{p}}) &= \alpha''_{1ij} \pm \alpha^{(3)\prime}_{1ijZ}(E_0^{(\mathrm{p})2})_Z \,,\end{aligned}\right\} \tag{59}$$

and

$$\left.\begin{aligned}\alpha'_{2ij}(\boldsymbol{E}_{\mathrm{p}}) &= \alpha'_{2ij} \mp \alpha^{(3)\prime\prime}_{2ijZ}(E_0^{(\mathrm{p})2})_Z \,, \\ \alpha''_{2ij}(\boldsymbol{E}_{\mathrm{p}}) &= \alpha''_{2ij} \pm \alpha^{(3)\prime}_{2ijZ}(E_0^{(\mathrm{p})2})_Z \,,\end{aligned}\right\} \tag{60}$$

respectively, explicitly writing out the real and imaginary components in each case.

Using eqs. (59) and (60) in the core equations finally provides the following measurables of class one spin chiral dichroism, using the example of eqs. (52) and (53).

The axial birefringence generated by switching the power laser from left to right circular polarity is

$$\langle (n_{\uparrow\uparrow \mathrm{L}} - n_{\uparrow\uparrow \mathrm{R}}) \rangle = -2\mu_0 c N (E_0^{(\mathrm{p})2})_Z \langle \alpha^{(3)\prime\prime}_{2XYZ} \rangle \,, \tag{61}$$

which depends on the square of $E_0^{(\mathrm{p})}$ and is proportional to the odd-parity component $\langle \alpha^{(3)\prime\prime}_{2XYZ} \rangle$. As in section 2, this class one effect conserves parity only in chiral ensembles. If observed in achiral ensembles it would be a sign of P violation. Being proportional to $E_0^{(\mathrm{p})2}$, which can reach 10^{20} $(\mathrm{V/m})^2$ in a focussed giant ruby laser, it is potentially a big effect, and therefore sensitive to P violation.

The corresponding axial dichroism in the power absorption coefficient measured by the probe is

$$\langle (A^{\mathrm{axial}}_{\uparrow\uparrow \mathrm{L}} - A^{\mathrm{axial}}_{\uparrow\uparrow \mathrm{R}}) \rangle = 4\omega\mu_0 N (E_0^{(\mathrm{p})2})_Z \langle \alpha^{(3)\prime}_{2XYZ} \rangle \,, \tag{62}$$

and has the same parity characteristics as the axial birefringence.

The circular birefringence, produced by switching the power laser from left to right polarisation, and measured with a plane polarised probe, is

$$\langle \theta_{\uparrow\uparrow \mathrm{L}} - \theta_{\uparrow\uparrow \mathrm{R}} \rangle = 4\mu_0 c^2 N \epsilon_0'^{1/2} E_{0Z}^{(\mathrm{p})2} \langle \alpha^{(3)\prime}_{1XYZ} \rangle \,, \tag{63}$$

and the circular dichroism in the power absorption coefficient, measured with the probe and produced by switching the power laser from left to right is given by

$$\langle A^{\mathrm{circ}}_{\uparrow\uparrow \mathrm{L}} - A^{\mathrm{circ}}_{\uparrow\uparrow \mathrm{R}} \rangle = 8\omega\mu_0 c N \epsilon_0'^{1/2} E_{0Z}^{(\mathrm{p})2} \langle \alpha^{(3)\prime\prime}_{1XYZ} \rangle \,. \tag{64}$$

Both effects are mediated by even-parity tensor components, and therefore conserve P in achiral and chiral ensembles. The same is true for the difference in rotation angle generated by the left to right switch of the power laser and measured by a plane polarised probe

$$\langle \Theta_{\uparrow\uparrow \mathrm{L}} - \Theta_{\uparrow\uparrow \mathrm{R}} \rangle = 2l\mu_0 N \omega \epsilon_0'^{1/2} c E_{0Z}^{(\mathrm{p})2} \langle \alpha^{(3)\prime}_{1XYZ} \rangle \,. \tag{65}$$

5.3.4. Class two spin chiral effects

Class two spin chiral effects are generated by switching the direction of a probe from Z to $-Z$, from parallel to antiparallel with respect to either a left or a right circularly polarised power laser. Axial effects use an unpolarised probe, as usual, and circular effects a circularly polarised or plane polarised probe. The mechanism responsible for class two effects is summarised in the conjugate products:

$$\boldsymbol{\Pi}_2 = \boldsymbol{E}_{\mathrm{L}}^{+(\mathrm{p})} \times \boldsymbol{B}_{\mathrm{L}}^{-(\mathrm{p})} = \boldsymbol{E}_{\mathrm{R}}^{+(\mathrm{p})} \times \boldsymbol{B}_{\mathrm{R}}^{-(\mathrm{p})} = 2E_0^{(\mathrm{p})} B_0^{(\mathrm{p})} \boldsymbol{k} \,, \tag{66}$$

which produce the following effects on the polarisabilty and optical activity tensors:

$$\left.\begin{aligned} \alpha'_{1ij}(\boldsymbol{E}^{(\mathrm{p})}, \boldsymbol{B}^{(\mathrm{p})}) &= \alpha'_{1ij} \pm \alpha^{(4)\prime}_{1ijZ}(E_0^{(\mathrm{p})} B_0^{(\mathrm{p})})_Z \,, \\ \alpha''_{1ij}(\boldsymbol{E}^{(\mathrm{p})}, \boldsymbol{B}^{(\mathrm{p})}) &= \alpha''_{1ij} \pm \alpha^{(4)\prime\prime}_{1ijZ}(E_0^{(\mathrm{p})} B_0^{(\mathrm{p})})_Z \,, \end{aligned}\right\} \tag{67}$$

$$\left.\begin{aligned} \alpha'_{2ij}(\boldsymbol{E}^{(\mathrm{p})}, \boldsymbol{B}^{(\mathrm{p})} &= \alpha'_{2ij} \pm \alpha^{(4)\prime}_{2ijZ}(E_0^{(\mathrm{p})} B_0^{(\mathrm{p})})_Z \,, \\ \alpha''_{2ij}(\boldsymbol{E}^{(\mathrm{p})}, \boldsymbol{B}^{(\mathrm{p})}) &= \alpha''_{2ij} \pm \alpha^{(4)\prime\prime}_{2ijZ}(E_0^{(\mathrm{p})} B_0^{(\mathrm{p})})_Z \,. \end{aligned}\right\} \tag{68}$$

Using these expressions in the core equations produces the following observables.

The axial birefringence for an unpolarised probe parallel and antiparallel to a left or right circularly polarised power laser is

$$\langle (n_{\Uparrow \mathrm{L}} - n_{\Downarrow \mathrm{L}}) \rangle = 2\mu_0 c N (E_0^{(\mathrm{p})} B_0^{(\mathrm{p})})_Z \langle \alpha^{(4)\prime}_{2XYZ} \rangle \,, \tag{69}$$

i.e., is mediated by an even-parity tensor component $\langle \alpha^{(4)\prime}_{2XYZ} \rangle$. This effect conserves P therefore in achiral and chiral ensembles. The corresponding axial dichroism is

$$\langle (A^{\mathrm{axial}}_{\Uparrow \mathrm{L}} - A^{\mathrm{axial}}_{\Downarrow \mathrm{L}}) \rangle = 4\omega\mu_0 N (E_0^{(\mathrm{p})} B_0^{(\mathrm{p})})_Z \langle \alpha^{(4)\prime\prime}_{2XYZ} \rangle \,, \tag{70}$$

with the same parity characteristics, in agreement with section 2.

In this case the circular birefringence difference is mediated by the odd-parity tensor component $\langle \alpha^{(4)\prime\prime}_{1XYZ} \rangle$, and conserves parity only in a chiral ensemble,

$$\langle \theta_{\Uparrow \mathrm{L}} - \theta_{\Downarrow \mathrm{L}} \rangle = 4\mu_0 c^2 N \epsilon_0'^{1/2} (E_0^{(\mathrm{p})} B_0^{(\mathrm{p})})_Z \langle \alpha^{(4)\prime\prime}_{1XYZ} \rangle \,, \tag{71}$$

the corresponding circular dichroism is

$$\langle A^{\mathrm{circ}}_{\Uparrow \mathrm{L}} - A^{\mathrm{circ}}_{\Downarrow \mathrm{L}} \rangle = -8\omega\mu_0 c N \epsilon_0'^{1/2} (E_0^{(\mathrm{p})} B_0^{(\mathrm{p})}) \langle \alpha^{(4)\prime}_{1XYZ} \rangle \tag{72}$$

and the difference in the angle of rotation of a plane polarised probe is

$$\langle \Theta_{\Uparrow \mathrm{L}} - \Theta_{\Downarrow \mathrm{L}} \rangle = 2l\mu_0 N \omega \epsilon_0'^{1/2} c (E_0^{(\mathrm{p})} B_0^{(\mathrm{p})}) \langle \alpha^{(4)\prime\prime}_{1XYZ} \rangle \,, \tag{73}$$

with the same P characteristics. Again, this is consistent with the analysis of section 2. The last observable, for example, is measured with a plane polarised probe parallel and antiparallel to either a right or a left circularly polarised power laser, such as a focussed giant ruby laser. This is particularly interesting for the potential evaluation of P violation in achiral ensembles, utilising the fact it is much larger in magnitude than class two axial birefringence and depends on the product of $E_0^{(\mathrm{p})}$ and $B_0^{(\mathrm{p})}$ of the power laser.

In summary, the core equations give new observables which depend on mediating tensor components whose symmetries are consistent in every case with the arguments of section 2.

5.3.5. Order of magnitude estimates

The Faraday effect is well measured, and the order of magnitude of the Wagnière–Meier effect has been estimated [20] to be about 10^{-7}, just within reach of a Rayleigh refractometer. Circular

birefringence due to a time varying electric field conserves P in chiral ensembles. However, it has apparently never been measured, although this is possible with contemporary fast response detector systems (such as a nanosecond Rollin detector), and an electric field alternating at mains frequencies (Hz range), orders of magnitude slower than the detector. With this type of apparatus axial birefringence due to an alternating electric field can also be measured and the following is an estimate of the magnitude of the latter effect for a reasonable value of the quantity $\langle \alpha^{(E)\prime}_{2XYZ} \rangle$.

Taking eq. (47), using $N = 6.0 \times 10^{26}$ molecules/m^3, $\mu_0 = 4\pi \times 10^{-7}$ J s^2 C^{-2} m^{-1}, $c = 3 \times 10^8$ m s^{-1}, we write the isotropic average [20] of the mediating tensor $\langle \alpha^{(E)\prime}_{2XYZ} \rangle$ in terms of the Levi–Civita tensor $\epsilon_{\alpha\beta\gamma}$ using the appropriate third rank isotropic average [20]. This produces the result

$$\langle (n_{\uparrow\uparrow} - n_{\uparrow\downarrow})_{E_Z(t)} \rangle = \mu_0 c N \dot{E}_Z(t) (\tfrac{1}{6} \epsilon_{\alpha\beta\gamma} (\alpha^{(E)\prime}_{2\alpha\beta\gamma} + \alpha_{2\alpha\beta} \mu_{E\gamma}/kT)) , \tag{74}$$

where $\boldsymbol{\mu}_E$ is the permanent electric dipole moment of the sample, which is partially aligned by $\boldsymbol{E}_Z(t)$, in analogy with dielectric relaxation [30]. The second term in the above equation allows for this alignment [20]. Using $\mu_{E\gamma} = 10 \times 10^{-30}$ C m; $kT = 4 \times 10^{-21}$ J; and a value for $\alpha_{2\alpha\beta}$ of 10^{-34} J^{-1} C^2 s^{-1} m^3 [20], we find for an electric field strength of 10^6 V m^{-1} that the axial birefringence produced by the alternating electric field is of the order of 10^{-8}. This is measurable in a Rayleigh refractometer [20], with electrodes in each arm to generate the electric field.

Circular birefringence due to a static magnetic field is several orders of magnitude greater than the equivalent axial effect, and is, of course, easily observable as the Faraday effect. Similarly, alternating electric field induced circular birefringence is expected from eq. (49) to be a much larger effect than the axial birefringence estimated above.

However, the biggest effects are expected from pulses of focussed giant ruby or Nd:YAG laser radiation in class one and class two spin chiral birefringence/dichroism. These are exemplified by isotropically averaging eq. (63), using the Rayleigh refringent scattering theory [20] and producing

$$\Delta\theta = \tfrac{1}{6} \omega \mu_0 c l N E^2_{0Z} \alpha''_{1\alpha\beta} \alpha''_{1\alpha\beta}/kT + \cdots , \tag{75}$$

an effect which is proportional to the electric field strength squared of the power laser pulse. In a small, commercially available Nd:YAG laser this can reach about 10^{18} (V/m)^2. The alignment effect of this can either be measured through the Kielich function [31] or from eq. (75). Taking an angular frequency of the probe, ω, of 10^{15} rad s^{-1} and a conservative order of magnitude of 10^{-38} J^{-1} C^2 m^2 for the imaginary part of the polarisability, $\alpha''_{1\alpha\beta}$, we arrive at

$$\Delta\theta \approx 10^{-12} E^2_{0Z} \text{ rad m}^{-1} ,$$

which for a conservative Nd:YAG pulse electric field strength of 10^6 V m^{-1} is 1 rad per meter of sample.

Similar estimates can be made for the axial birefringence due to class one dichroism, leading to

$$\langle n_{\uparrow\uparrow L} - n_{\uparrow\uparrow R} \rangle \approx 10^{-23} E^2_{0Z} \tag{76}$$

for an order of magnitude estimate [20] of 10^{-34} A^2 J^{-1} m^3 s for the appropriate part of the Rosenfeld tensor, $\alpha_{2\alpha\beta}$. For a Q switched and focussed Nd:YAG laser delivering up to 10^9 V m^{-1}, this produces an axial birefringence in chiral media only of about 10^{-5}, within the range of a Rayleigh refractometer.

6. Parity violation in class one and class two spin chiral birefringence/dichroism

In this section is is assumed that there exist intrinsically P violating mediating tensors, whose origins reside in the theory of weak neutral current interactions [32]. On this basis, eq. (61) becomes

$$\langle n_{\uparrow\uparrow L} - n_{\uparrow\uparrow R} \rangle_{PV} = -2\mu_0 cNE_{0Z}^{(p)2} \langle \alpha_{2XYZ}^{(3)\prime\prime} \rangle_{PV} , \tag{77}$$

where the subscript PV indicates "intrinsically parity violating". Equation (77) implies that class one spin chiral axial birefringence would be observable in an *achiral* ensemble, and would be a direct measure of the magnitude of P violation in the molecular ensemble. The effect is proportional to the square of $E_0^{(p)}$ and to the ensemble average of the P violating totally antisymmetric tensor element $\langle \alpha_{2XYZ}^{(3)\prime\prime} \rangle_{PV}$.

Similarly, eq. (73) becomes

$$\langle \Theta_{\uparrow\uparrow L} - \Theta_{\uparrow\downarrow L} \rangle_{PV} = 2l\mu_0 N\omega\epsilon_0'^{1/2} c(E_0^{(p)} B_0^{(p)})_Z \langle \alpha_{1XYZ}^{(4)\prime\prime} \rangle_{PV} , \tag{78}$$

which can be rewritten using eq. (43) as

$$\langle \Theta_{\uparrow\uparrow L} - \Theta_{\uparrow\downarrow L} \rangle_{PV} = 2l\mu_0 N\omega E_{0Z}^{(p)2} \langle \alpha_{1XYZ}^{(4)\prime\prime} \rangle_{PV} . \tag{79}$$

This is the difference in rotation angle measured by a plane polarised probe parallel and antiparallel to a right or left circularly polarised power laser in an *achiral* ensemble. Such a measurable would be a direct indication of P violation, and would be proportional to the sample length l multiplied by the square of $E_0^{(p)}$ of the power laser. By maximising l and $E_0^{(p)2}$ for a given achiral ensemble, the observable can be made sensitive to P violation.

To estimate the magnitude of the P violating ensemble average $\langle \alpha_{1XYZ}^{(4)\prime\prime} \rangle_{PV}$ in eq. (78) requires ab initio computation of the type first used by Mason and Tranter [33], using the quantum perturbation expressions for molecular property tensors described, for example, by Wagnière and Hutter [34]. This computation can be achieved in principle with a contemporary software package such as HONDO [35]. Optical rotations have been observed in achiral atomic ensembles [36], and estimates of the P violating enantiomeric energy inequivalence have been given by Mason and Tranter [33].

7. A configuration for the measurement of reversality violation

The violation of reversality follows theoretically [37] from the experimental observation of P violation. An experimental configuration for the direct observation of T violation can be suggested from the basic symmetry arguments of section 2. It has been shown there that both axial and circular birefringence observed with a time varying magnetic field, or a static electric field, would measure T violation in principle. However, the available data from nuclear physics [38] indicate that T violation is an extremely small effect, needing a configuration of maximum sensitivity. The currently available magnetic and electric field strengths are unlikely to be able to provide this degree of sensitivity, implying that intense laser fields are necessary.

In this context the P violating configurations of section 6 can be adapted in principle for T violation by employing an additional static electric field, so that the double Taylor expansion (15) becomes a triple Taylor expansion, with additional dependence of the polarisability and optical activity tensors on the static electric field. This would have the effect of making the T violating observable proportional to

the square of $E_0^{(p)}$ multiplied by the static electric field strength, thus greatly amplifying the sensitivity of the experimental configuration. The latter would still retain simplicity, being made up simply of two lasers passing through a sample with additional electrodes generating a static electric field.

8. Computer simulation: "hidden variable" dynamics

In this section a molecular dynamics computer simulation is used to investigate the dynamical effect of class one spin chiral dichroism in a chiral sample of 108 S bromochlorofluoromethane molecules interacting with a site potential described elsewhere [39]. The simulation method utilised the Cornell National Supercomputer Facility's IBM 3090-6S supercomputer to integrate, using parallel FORTRAN, the equations of motion of the sample in the presence of an extra torque due to the cross product (57) of the electric field components of the power laser. The form of this torque has been detailed elsewhere [40], and contains a real component even though the product (57) is purely imaginary, and whose polarisation effect, therefore, is not directly observable, as discussed by Wagnière with quantum perturbation theory [41]. The simulation shows that the real component of the torque gives rise to clear spectral (bandshape) effects, which are frequency dependent, and play a role in the axial and circular birefringence effects of class one, discussed in section 5. This type of effect is classified here as "hidden variable" dynamics, which accompanies class one spin chiral dichroism/birefringence through the ensemble-averaged torque [42]

$$\langle \boldsymbol{T}_q \rangle = \langle \text{Hyperpolarisability } (\boldsymbol{E}_L^{+(p)} \times \boldsymbol{E}_L^{-(p)}) \times \boldsymbol{E}_L^{(p)} \rangle \, . \tag{80}$$

Incorporation of this in the simulation algorithm TETRA [40] took place in the forces loop and after re-equilibration, time auto- and cross-correlation functions of the dynamics were evaluated using contiguous segments at two power laser frequencies, 10.0 and 0.01 THz, in the far-infrared range. The time step of the simulation was 50.0 fs, and was carried out at 293 K, 1.0 bar.

It was observed numerically that anisotropy developed in the characteristic time correlation functions of the ensemble, such as the orientational auto-correlation function (acf) measured by an axis in the net electric molecular dipole moment ($\boldsymbol{\mu}$). This became more pronounced at the lower power laser field frequency, and is therefore relaxational in nature. The anisotropy was accompanied by the development in the laboratory frame of orientational cross-correlation functions (ccf) [39] between different (off-diagonal) Cartesian elements of the tensor product $\langle \boldsymbol{\mu}(t)\boldsymbol{\mu}(0) \rangle$. Four such elements were clearly isolated. These occur even though the polarisation due to (57) is purely imaginary.

Similar dynamical ensemble effects were observed with the rotational velocity cf matrix $\langle \dot{\boldsymbol{\mu}}(t)\dot{\boldsymbol{\mu}}(0) \rangle$, whose trace is the Fourier transform, essentially, of the far-infrared power absorption coefficient. These simulation results show clearly that spin chiral dichroism of class one is a molecular dynamical (relaxational) effect. In principle, therefore, it can be developed into a novel type of spectroscopy, giving very specific information on new molecular property tensors, and on "hidden variable" dynamics. The same conclusion holds for other effects given in section 5.

9. Experimental investigation

Finally, a method for the experimental investigation of these effects is given, based on Rayleigh's refractometer [43], an instrument which has a refractive index sensitivity of up to one part in 10^8.

9.1. Static magnetic field

As first suggested by Barron and Vrbancich [20], the magnetic fields are generated in different directions in the two arms of Rayleigh's refractometer, with the probe sent down each arm in the same direction, using a suitable [20] chiral sample. Superconducting techniques now enhance the static magnetic field strengths available. A configuration less susceptible to artifact might involve one magnet only, with the probe sent in opposite directions down the two arms from a single source.

9.2. Time varying electric field

The technique relies on a fast detector system for changes in the probe intensity caused by alternating the electric field at much lower frequencies, and is therefore a time-resolved technique on a scale dependent on the response of the detector system. The Rayleigh refractometer is used with the probe sent in the same direction down each arm, and with a positive and a negative electrode to generate the electric field. The polarity of the electrodes in the two arms is opposite, so that the alternating electric fields are out of phase. To maximise sensitivity, the sample is highly dipolar, and the arm length restricted to about 10.0 mm for maximisation of electric field strength. The transient effect on the probe reaching a fast detector system is measured on the nanosecond scale with an alternating electric field at around mains frequencies.

Circular dichroism in a chiral sample due to an alternating electric field is picked up dynamically with a fast detector, such as a helium-cooled Rollin, and a right or left circularly polarised probe.

9.3. Electromagnetic effects

The class one and two spin chiral effects discussed in section four are time independent, because they are due to conjugate products which remove the phases of the power laser components. They do not need time-resolved apparatus therefore, and can be detected at equilibrium with a combination of probe and power lasers.

Acknowledgements

This research was conducted using the resources of the Center for Theory and Simulations in Science and Engineering (Cornell Theory Center), which receives major funding from the National Science Foundation and IBM Corporation, with additional support from New York State and members of the Corporate Research Institute.

Apendix A

Conservation of reversality

Reversality is most accurately defined as motion reversal, which leaves position vectors unchanged but which reverses all motions (conjugate momenta). Time can be defined in the nonrelativistic approximation as position divided by linear velocity, so reversality changes t to $-t$. In this appendix we discuss further the notation of the symmetry panels used in the text. A good discussion of reversality is given in refs. [5] and [16].

According to Wigner's symmetry principles [16], a reversality conserving complete experiment is positive to T. In the generation of the Faraday effect or magnetochiral dichroism, the essential symmetry characteristic [9] is described diagramatically as below:

$$\begin{array}{ccc} \left\{\begin{array}{l}\rightarrow \boldsymbol{B}\\ \rightarrow \boldsymbol{K}_{\mathrm{p}}\end{array}\right\} & \text{compared} & \left\{\begin{array}{l}\leftarrow -\boldsymbol{B}\\ \rightarrow \boldsymbol{K}_{\mathrm{p}}\end{array}\right\} \\ \downarrow T & & \downarrow T \\ \left\{\begin{array}{l}\leftarrow -\boldsymbol{B}\\ \leftarrow -\boldsymbol{K}_{\mathrm{p}}\end{array}\right\} & \text{compared} & \left\{\begin{array}{l}\rightarrow \boldsymbol{B}\\ \leftarrow -\boldsymbol{K}_{\mathrm{p}}\end{array}\right\} \end{array} ,$$

i.e. the measured variable is different with $\boldsymbol{B}$ parallel and antiparallel to the propagation vector ($\boldsymbol{K}_{\mathrm{p}}$) of the probe. In both cases the following holds:

$$[\Gamma(\boldsymbol{B})\Gamma(\boldsymbol{K}_{\mathrm{p}})] \overset{T}{\rightarrow} + [\Gamma(-\boldsymbol{B})\Gamma(-\boldsymbol{K}_{\mathrm{p}})] , \tag{A.1}$$

i.e. the motion reversal (T) symmetry of the product $\boldsymbol{B}\cdot\boldsymbol{K}_{\mathrm{p}}$ is positive. Panel 3 of the text incorporates this with the other variables of the complete Faraday effect and magnetochiral experiments.

In the case of a time varying electric field, the same considerations hold with $\boldsymbol{E}(t)$ substituted for $\boldsymbol{B}$. To illustrate what is meant by a time varying electric field, it is helpful to exemplify with specific functional forms for $\boldsymbol{E}(t)$. For example, if the apparatus is designed to produce

$$\boldsymbol{E}(t) = E_0 \sin(\omega t) , \tag{A.2}$$

where ω is the alternating frequency, we must consider the T symmetry of the function $\boldsymbol{E}(t)$. The quantity E_0 is a scalar electric field strength amplitude in $\mathrm{V\,m^{-1}}$, and is motion independent and T positive. Similarly, ω is a scalar angular frequency, in rad/s, a number which is unchanged by T. Finally, as we have seen, t is changed by T to $-t$. The function $E_0 \sin(\omega t)$ is *negative* to T, therefore, using the property of the sine function.

If, on the other hand, the apparatus produces

$$\boldsymbol{E}_1(t) = E_0 \cos(\omega t) , \tag{A.3}$$

the function $\boldsymbol{E}(t)$ itself is T positive, but its time derivative

$$\begin{aligned} \dot{\boldsymbol{E}}_1(t) &= -\omega E_0 \sin(\omega t) \\ &= -\omega E_0 \cos(\omega t - \pi/2) , \end{aligned} \tag{A.4}$$

$$\dot{\boldsymbol{E}}_1(t) \overset{T}{\rightarrow} -\dot{\boldsymbol{E}}_1(t) \tag{A.5}$$

is T negative. This derivative may be used in eqs. (13) and (14) to give eqs. (47)–(51) of the text. Clearly, with a field of the type (A.3) we could equally as well have used $\dot{\boldsymbol{E}}_1(t)$ in the Voigt–Born perturbation theory.

Therefore, the electric field equivalent of the Faraday and magnetochiral effects varies with the functional dependence on t of the applied electric field, called in the text a "time dependent electric field".

Diagrams (5) and (6) of the text consider class one and class two spin chiral effects, first introduced in ref. [9]. For class one, the conservation of reversality is described essentially by

$$[\Gamma(\boldsymbol{\Pi}_{1R})\Gamma(\boldsymbol{K}_p)] \xrightarrow{T} + [\Gamma(-\boldsymbol{\Pi}_{1L})\Gamma(-\boldsymbol{K}_p)] , \qquad \boldsymbol{K}_R \xrightarrow{T} -\boldsymbol{K}_L , \tag{A.6}$$

where $\boldsymbol{K}_R$ and $\boldsymbol{K}_L$ are the propagation vectors of the right and left circularly polarised power (or "pump") laser, $\boldsymbol{\Pi}_{1R}$ and $\boldsymbol{\Pi}_{1L}$ are the conjugate products (57) (see section 5.3.3) of the text for this laser, and $\boldsymbol{K}_p$ is the propagation vector of the linearly or unpolarised probe laser directed along the same axis as the pump, similar, for example, to the apparatus used in the optical Kerr effect. This can be summarised diagrammatically by

$$\begin{Bmatrix} \rightarrow \boldsymbol{K}_L \\ \rightarrow \boldsymbol{\Pi}_{1L} \\ \rightarrow \boldsymbol{K}_p \end{Bmatrix} \text{ compared with } \begin{Bmatrix} \rightarrow \boldsymbol{K}_R \\ \leftarrow -\boldsymbol{\Pi}_{1R} \\ \rightarrow \boldsymbol{K}_p \end{Bmatrix}$$

$$\downarrow T \qquad\qquad \downarrow T$$

$$\begin{Bmatrix} \leftarrow -\boldsymbol{K}_R \\ \leftarrow -\boldsymbol{\Pi}_{1R} \\ \leftarrow \boldsymbol{K}_p \end{Bmatrix} \text{ compared with } \begin{Bmatrix} \leftarrow -\boldsymbol{K}_L \\ \rightarrow \boldsymbol{\Pi}_{1L} \\ \leftarrow -\boldsymbol{K}_p \end{Bmatrix} .$$

This diagram means that an observable birefringence and dichroism is generated by switching the circular polarity of the pump, keeping constant the directions of both pump and probe.

To understand the effect of T in this diagram, recall that right circular polarity is defined as the clockwise rotational motion of the electric field vector of the electromagnetic field, and T converts this to anticlockwise motion, i.e. changes R to L. Specifically,

$$\boldsymbol{E}_L^+ \xrightarrow{T} \boldsymbol{E}_R^- , \qquad \boldsymbol{E}_L^- \xrightarrow{T} \boldsymbol{E}_R^+ , \qquad \boldsymbol{E}_R^+ \xrightarrow{T} \boldsymbol{E}_L^- ; \qquad \boldsymbol{E}_R^- \xrightarrow{T} \boldsymbol{E}_L^+ ,$$

$$(\boldsymbol{E}_L^+ \times \boldsymbol{E}_L^-) \xrightarrow{T} (\boldsymbol{E}_R^- \times \boldsymbol{E}_R^+) = -(\boldsymbol{E}_R^+ \times \boldsymbol{E}_R^-) ,$$

$$\boldsymbol{\Pi}_{1L} \xrightarrow{T} -\boldsymbol{\Pi}_{1R} , \tag{A.7}$$

and it follows from eq. (A.7) and the above diagram that class one spin chiral effects conserve reversality.

Finally, class two spin chiral effects differ from class one in that the direction of the pump laser is reversed relative to that of the probe, but its circular polarity is kept constant. This is summarised diagrammatically as follows:

$$\begin{Bmatrix} \rightarrow \boldsymbol{K}_{L,R} \\ \rightarrow \boldsymbol{\Pi}_{2L,R} \\ \rightarrow \boldsymbol{K}_p \end{Bmatrix} \text{ compared with } \begin{Bmatrix} \leftarrow \boldsymbol{K}_{L,R} \\ \leftarrow -\boldsymbol{\Pi}_{2L,R} \\ \rightarrow \boldsymbol{K}_p \end{Bmatrix}$$

$$\downarrow T \qquad\qquad \downarrow T$$

$$\begin{Bmatrix} \leftarrow -\boldsymbol{K}_{R,L} \\ \rightarrow \boldsymbol{\Pi}_{2R,L} \\ \leftarrow -\boldsymbol{K}_p \end{Bmatrix} \text{ compared with } \begin{Bmatrix} \rightarrow \boldsymbol{K}_{R,L} \\ \leftarrow -\boldsymbol{\Pi}_{2R,L} \\ \leftarrow -\boldsymbol{K}_p \end{Bmatrix} .$$

In this case note that the relevant conjugate product (66) is independent of the circular polarity of the pump laser, which is kept constant, but reverses sign if the forward motion of the pump laser is changed to backward motion.

To summarise, class one effects are generated by keeping the relative directions of the pump and probe the same, and switching the circular polarity of the pump, thereby reversing the sign of the conjugate product vector (57) for fixed $\boldsymbol{k}$, i.e. $\boldsymbol{k}$ always positive, or always negative, relative to the probe. T in this case reverses all three vectors (the pump and probe propagation vector, and the

conjugate product vector (57)). All three remain *relatively* the same (*relatively* T positive) in the motion-reversed experiment. Class two effects are generated by switching the relative directions of the pump and probe, using a conjugate product vector (66) which is independent of the circular polarity of the pump but which reverses sign for $\boldsymbol{k} \rightarrow -\boldsymbol{k}$, equivalent to switching the pump laser from forward to backward motion relative to the probe. T again reverses the propagation vectors of the pump and probe but the conjugate product $\boldsymbol{\Pi}_2$ (eq. (66)) is unchanged by T. The original experiment generates observables by changing the sign of the dot product $\boldsymbol{K}_{R,L} \cdot \boldsymbol{K}_p$ of the two propagation vectors and also changing the sign [44] of $\boldsymbol{\Pi}_2$, because $\boldsymbol{k}$ is changed to $-\boldsymbol{k}$ in the pump laser, whose direction is reversed. The motion-reversed experiment generates the observables relatively in the same way and therefore conserves reversality.

Appendix B

Results from Rayleigh refringent scattering theory

Semiclassical Rayleigh refringent scattering theory [20] has been applied to magnetochiral dichroism and birefringence. This has been used to produce the result (74) of section 5, where the property tensors were expressed *in the molecular fixed frame* for a sinusoidal electric field $\boldsymbol{E}(t)$. It has also been used to derive eq. (75) for circular birefringence due to class one spin chiral effects, showing that this is easily observable, in principle, with a moderate pump laser electric field strength. The molecular property tensors in eq. (75) are again expressed in the molecule fixed frame of reference.

Note added in proof

The author thanks Professor S. Woźniak for a copy of S. Woźniak and R. Zawodny, Acta Phys. Pol. A 61 (1982) 175, in which an expression is derived for magnetochiral dichroism, and called "magneto-spatial dispersion". The Wagnière–Meier effect can also be referred to, therefore, as the Woźniak–Zawodny effect.

References

[1] P.G.H. Sandars, in: Fundamental Interactions and Structure of Matter, eds. K. Crowe, J. Duclos, G. Fiorentini and G. Torelli (Plenum, New York, 1980) p. 57.
[2] E.N. Fortson and L. Wilets, Adv. At. Mol. Phys. 16 (1980) 319.
[3] M. Forte, B.R. Heckel, N.F. Ramsey, K. Green, G.J. Greene, J. Byrne and J. Pendlebury, Phys. Rev. Lett. 45 (1980) 2088.
[4] For a review, see L.D. Barron, Chem. Soc. Rev. 15 (1986) 189.
[5] L.D. Barron, Fundamental symmetry aspects of molecular chirality, in: New Developments in Molecular Chirality, ed. P.G. Mezey (Reidel, Amsterdam, 1990).
[6] P.W. Anderson, Basic Notions of Condensed Matter Physics (Benjamin/Cummins, Menlo Park, 1983).
[7] A.O. Barut, Found. Phys. 13 (1983) 7.
[8] M. Quack, Angew. Chem. Int. Ed. Engl. 28 (1989) 571.
[9] M.W. Evans, Chem. Phys. Lett. 152 (1988) 33.
[10] M.W. Evans, Chem. Phys. 132 (1989) 1.
[11] S.F. Mason, Molecular Optical Activity and the Chiral Discriminations (Cambridge Univ. Press, 1982).
[12] M.W. Evans, Mol. Phys. 67 (1989) 1195.
[13] C. Charney, The Molecular Basis of Optical Activity (Wiley, New York, 1979).

See D.C. Cheng and G.K. O'Neill, Elementary Particle Physics (Addison-Wesley, Reading 1979).
T.D. Lee and C.N. Yang, Phys. Rev. 104 (1956) 254.
For example, L.D. Barron, Molecular Light Scattering and Optical Activity (Cambridge Univ. Press, 1982).
G. Wagnière and A. Meier, Chem. Phys. Lett. 93 (1982) 78.
G. Wagnière and A. Meier, Experientia 39 (1983) 1090.
G. Wagnière, Z. Naturforsch. A 39 (1984) 254.
L.D. Barron and J. Vrbancich, Mol. Phys. 51 (1984) 715.
P.W. Atkins, Molecular Quantum Mechanics (Oxford Univ. Press, 1983).
L.D. Landau and E.M. Lifshitz, Electrodynamics of Continuous Media, (Pergamon, Oxford, 1960).
M.W. Evans, Phys. Lett. A 134 (1989) 409; 146 (1990) 185, 485.
M.W. Evans, Phys. Rev. A 39 (1989) 6041.
M.W. Evans, Chem. Phys. Lett. 158 (1989) 375.
M.W. Evans, Chem. Phys. 135 (1989) 187.
See Symmetry analysis, ref. [9].
R.L. Flurry, Jr., Symmetry Groups, Theory and Chemical Applications (Prentice-Hall, Englewood Cliffs, 1980).
Y.R. Shen, The Principles of Non-Linear Optics (Wiley, New York, 1984).
M.W. Evans, G.J. Evans, W.T. Coffey and P. Grigolini, Molecular Dynamics (Wiley Interscience, New York, 1982).
S. Kielich, in: Dielectric and Related Molecular Processes, ed. M. Davies Vol. 1 (Chem. Soc. London, 1972).
S. Weinberg, Phys. Rev. Lett. 19 (1967) 1264.
S.F. Mason and G.E. Tranter, Proc. R. Soc. London A 397 (1985) 45.
G. Wagnière and J.B. Hutter, J. Opt. Soc. Am. B 6 (1989) 695.
E. Clementi, ed., MOTECC 89 (ESCOM, Leiden, 1989).
M.A. Bouchiat and L. Pottier, Sci. Am. 250(6) (1984) 76.
V.B. Beresteskii, E.M. Lifshitz and L.P. Pitaevski, Quantum Electrodynamics (Pergamon, Oxford, 1982).
J.H. Christenson, J.W. Cronin, V.L. Fitch and R. Turlay, Phys. Rev. Lett. 13 (1964) 138.
M.W. Evans, G.C. Lie and E. Clementi, Z. Phys. D 7 (1988) 397.
M.W. Evans, Phys. Rev. Lett. 64 (1990) 2909; Opt. Lett. 15 (1990) 863.
G. Wagnière, Phys. Rev. A 40 (1989) 2437.
M.W. Evans and G. Wagnière, Phys. Rev. Lett., in press.
M. Born and E. Wolf, Principles of Optics (Pergamon, Oxford, 1975).
G. Wagnière, Z. Phys. D 8 (1988) 229.